Defence Science Journal, Vol. 71, No. 4, July 2021, pp. 564-571, DOI : 10.14429/dsj.71.16760

Tungsten Heavy Alloys with Two-phase Matrix

G. Prabhu[#,*], R. Arockia Kumar[@], and T.K. Nandy[#]

[#]*DRDO-Defence Metallurgical Research Laboratory, Hyderabad - 500 058, India*
[@]*National Institute of Technology, Warangal – 506 004, India*
[*]*E-mail: gprabhu@dmrl.drdo.in*

ABSTRACT

WNiCo alloys subjected to a two-stage or cyclic heat treatment develop a unique microstructure wherein apart from tungsten grains and matrix phase, fine tungsten precipitates are distributed in the matrix. This is unlike conventional heavy alloys such as WNiFe and WNiFeCo where the matrix is single phase without any secondary microstructural features. The purpose of developing a two-phase matrix is to realise superior mechanical properties compared to conventional alloys, especially strength with comparable or superior elongation and impact toughness. This advantage has rendered WNiCo alloys (with two-phase matrix) suitable candidates for advanced kinetic energy penetrators. The present study focusses on processing 92W-5Ni-3Co alloy using cyclic heat treatment and optimisation of parameters involved in cyclic heat treatment as well as subsequent vacuum heat treatment. Any refinement in processing parameters will help in improving the mechanical properties given the fact that processing parameters, microstructural features and mechanical properties are strongly interdependent in the case of tungsten heavy alloys.

Keywords: Tungsten heavy alloys; Cyclic heat treatment; Two-phase matrix; Tungsten precipitates

1. INTRODUCTION

Kinetic energy penetrators used as anti-tank ammunition are made of tungsten heavy alloys. These alloys consist of 88-95 wt% W and the balance is usually a combination of Ni, Fe and Co[1]. Though WNiFe and WNiFeCo alloys are well established alloy systems, WNiCo alloys are currently being considered for stringent applications such as penetrators mainly because of the superior properties achievable in these alloys[2]. Improvements in armour technology have also underlined the requirement for developing penetrators with enhanced ballistic performance. Hence, the present study aimed at processing WNiCo alloys gains significant relevance given the fact that these alloy systems are closely guarded with very limited literature available on their processing methodology.

Major difference between WNiFe/WNiFeCo alloys and WNiCo alloy lies in the matrix phase that holds the tungsten grains together; the matrix is single-phase in the case of WNiFe/WNiFeCo alloys and two-phase with fine micron-sized particles in WNiCo alloy. Tungsten heavy alloys have been studied extensively with the primary focus being on their suitability for critical applications and the matrix phase has always been a single-phase except in the case of oxide dispersed alloys. One of the major shortcomings of the single-phase matrix is the concomitant decrease in ductility (and impact toughness) observed while increasing strength levels using thermo-mechanical treatments. This poses a limitation on improving the strength and also restricting the scope for additional processing since reasonable amount of ductility is required for subsequent mechanical working. It is in this scenario that a two-phase matrix which has the potential to maintain strength as well as ductility even in the deformed condition gains importance over conventional single-phase matrices.

One of the early investigations that discusses improvement in strength while retaining ductility is proposed by Stuitje[2], *et al.* WNiCo alloy subjected to a two-stage or cyclic heat treatment develops tungsten precipitates in its matrix phase and such a two-phase matrix reportedly exhibits the advantages discussed above. This heat treatment cycle and the resultant microstructure are considered unique since conventional heat treatments do not result in such a two-phase matrix. It is for these facts that processing of WNiCo alloys is not widely reported and the only literature available on processing is by Stuitje[2], *et al.* Skoczylas[3], *et al.* have also mentioned that the presence of precipitates could be the reason behind the higher strength observed in 91W-6Ni-3Co alloy compared to a 91W-6Ni-2.25Fe-0.75Co alloy. Though processing details are not mentioned, it has been reported that the precipitates are most likely $(Ni,Co)_3W$ or $(Co,Ni)_7W_6$ intermetallic phases and they provide dispersion strengthening of the matrix phase[3]. Recently, Sarkar[4], *et al.* have also reported Co_2W intermetallic phase in 92W-5.3Ni-2.7Co alloy.

Authors earlier investigation using 92W-5Ni-3Co alloy brings out the advantages of cyclic heat treatment upon comparison with the same composition processed without cyclic heat treatment[5]. The present study however focusses varying the process parameters involved in cyclic and

Received : 01 February 2021, Revised : 08 April 2021
Accepted : 25 May 2021, Online published : 01 July 2021

subsequent vacuum heat treatment in order to vary the fraction of precipitates in the matrix and understand the effect of such a variation on the mechanical properties. This study focusses on mechanical properties in heat-treated condition since any improvement in heat-treated condition can be exploited beneficially and extended to subsequent mechanical working stages.

2. EXPERIMENTAL SETUP

Commercial grade tungsten, nickel and cobalt powders of 99.95% minimum purity and median particle size of 5, 8 and 4 μm respectively, are used for processing 92W-5Ni-3Co alloy (hereinafter referred to as 92W alloy). Mixing of powders was carried for 48 h in a ball mill using stainless steels balls as the mixing medium at a 1:1 Ball to Powder Ratio (BPR). The powder mix was then reduced at 700˚C for 2 h in hydrogen atmosphere using a reduction furnace (Make: Sintering and Brazing Furnaces Ltd, India) and compacted at 200 MPa using a cold isostatic press (Make: National Forge, Belgium). Pre-sintering at 1300˚C for 2 h followed by liquid phase sintering at 1490˚C for 1 h 15 minutes was carried out in hydrogen atmosphere using a sintering furnace (Make: FHD Furnaces Ltd, England).

Sintered samples were subjected to a post-sintering processing sequence as shown in Fig. 1a Cyclic or two-stage heat treatment (CHT) includes first stage treatment at 800˚C for 5 h followed by a second stage treatment at a higher temperature for 5 h, as shown in Fig. 1a. Second stage temperature was varied from 1050, 1100 to 1150˚C as shown in Fig. 1a and as listed in Table 1. CHT involving two continuous cycles is shown in Fig. 1b. Vacuum heat treatment (VHT) that follows CHT is also carried out at two different temperatures; at 1100˚C for 4 h in VHT 1 and at 1150˚C for 4 h in VHT 2, as shown in Fig. 1a.

Microstructural characterisation was carried out after CHT and after VHT 1 and 2 using scanning electron microscope (SEM Make: FEI, Quanta 400). Precipitates were characterised using transmission electron microscope (TEM Make: FEI Tecnai 20T G^2) and compositional analysis of precipitates was carried out using TEM Energy Dispersive Spectroscopy (EDS). Tungsten grain size, matrix volume fraction and fraction of precipitates were determined using ImageJ software. Dissolved tungsten in the matrix was determined using SEM EDS. Tensile and impact fractographs of failed samples were studied using scanning electron microscope.

Table 1. Process parameters used in the present study

CHT parameters		VHT 1	VHT 2
First stage	Second stage		
800˚C/5h	1050˚C/5h 1100˚C/5h 1150˚C/5h	1100˚C/4h	1150˚C/4h
[800˚C/5h -1150˚C/5h] - repeated twice as in Fig. 1b			

Tensile samples prepared as per ASTM standard E8-T11 (2003) were tested in a tensometer (Make: Monsanto, Capacity: 2000 kg). Charpy unnotched impact samples prepared as per ASTM E23-05 were tested in a pendulum type impact testing machine (Make: Fuel Instruments India, Model: IT 30 ASTM, 0 to 300 Joules).

3. RESULTS

Differential scanning calorimetry (DSC) trace of as-sintered 92W alloy shows exothermic peak around 800˚C and endothermic peaks around 1050˚C, 1250˚C, as shown in Fig. 2.

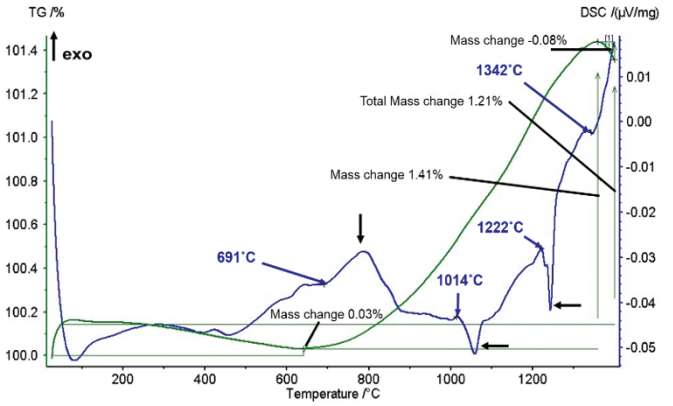

Figure 2. DSC plot of as-sintered 92W alloy. Exothermic and endothermic peaks and valleys are shown by arrows.

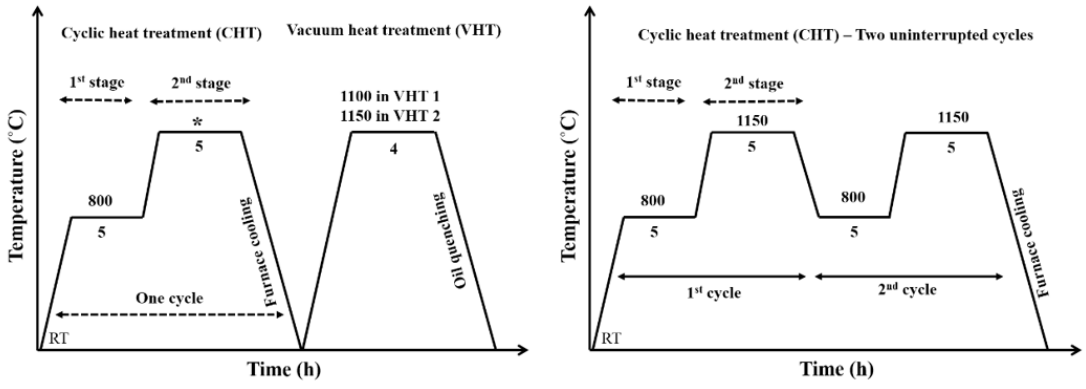

Figure 1. (a) Schematic of the post-sintering processing sequence followed in the present study. *Second stage temperature in CHT is varied from 1050, 1100 to 1150˚C and (b) CHT with two continuous cycles.

Microstructures of the alloy in cyclic heat-treated condition are shown in Fig. 3. As shown in Figs. 3a to 3d, the microstructure includes nearly-spherical tungsten grains, continuous matrix phase and tungsten precipitates in the matrix phase. In the case of 1050˚C being second stage temperature, tungsten precipitates in the matrix are of both elongated and nearly-spherical morphology (as shown in Fig. 3a, S-nearly-spherical and E - elongated) whereas after 1100 and 1150˚C, most of the tungsten precipitates are nearly-spherical as shown in Figs. 3b and c. After 2 continuous cycles as shown in Fig. 1b, morphology of the most of the precipitates remains nearly-spherical, as shown in Fig. 3d, but the fraction of precipitates has increased compared to those in Figs. 3b and c that correspond to single cycle treatments. TEM bright field images shown in Fig. 3e correspond to 1050˚C sample and reveal that the tungsten precipitates are of both nearly-spherical and elongated morphology. Selective area diffraction (SAD) patterns (Fig. 3e) confirm that the precipitates are tungsten.

Composition analysis carried out using TEM EDS, as listed in Table 2, further corroborates that the precipitates are rich in tungsten with only traces of nickel and cobalt.

Table 2. TEM EDS analysis of precipitates

	Spherical	Elongated
Element	wt %	wt %
W	97.9	93.2
Ni	1.5	4.4
Co	0.6	2.4
Total	100	100

Microstructures of 92W alloy in vacuum heat-treated condition (VHT 1 and 2) are similar to the microstructures shown in Fig. 3a to 3d except for the difference in volume fraction as listed in Tables 4 and 5. In terms of morphology of the precipitates, elongated precipitates are rarely observed, instead, the precipitates are of nearly-spherical morphology.

Microstructural parameters determined after CHT and VHT 1, 2 are listed in Table 3 to 5. Tungsten grain size and matrix volume fraction remain comparable between cyclic heat treatment and vacuum heat treatment, as shown in Fig. 4a. Marginal increase is observed in dissolved tungsten in CHT samples; 42.17 wt% after 1050ºC against 43.35 wt% after 1150ºC. Volume fraction of precipitates after CHT is lesser in the case of 1100 and 1150˚C compared to 1050˚C and 1150˚C/2 cycles as listed in Table 3 and shown in Fig. 4a. Further, the fraction of precipitates following VHT 1 and 2 are listed in Table 4 and 5. In both the cases, fraction of precipitates has decreased in 1050˚C-VHT (1 and 2) sample as compared to

Table 3. Microstructural parameters determined after CHT.

CHT parameters		Microstructural parameters after CHT		
First stage	Second stage	Grain size (µm)	Matrix vol. fraction (vol.%)	Vol. fraction of precipitates (%)
800˚C/5h	1050˚C/5h	27.7 ± 6.3	18.8 ± 2	4.7 ± 1
	1100˚C/5h	25.8 ± 9.1	17.5 ± 2.5	1.2 ± 0.7
	1150˚C/5h	24.8 ± 9.1	17.1 ± 2.4	1.1 ± 0.5
	1150˚C/5h (2 cycles)	24.1 ± 7.7	19.6 ± 0.4	3.8 ± 0.3

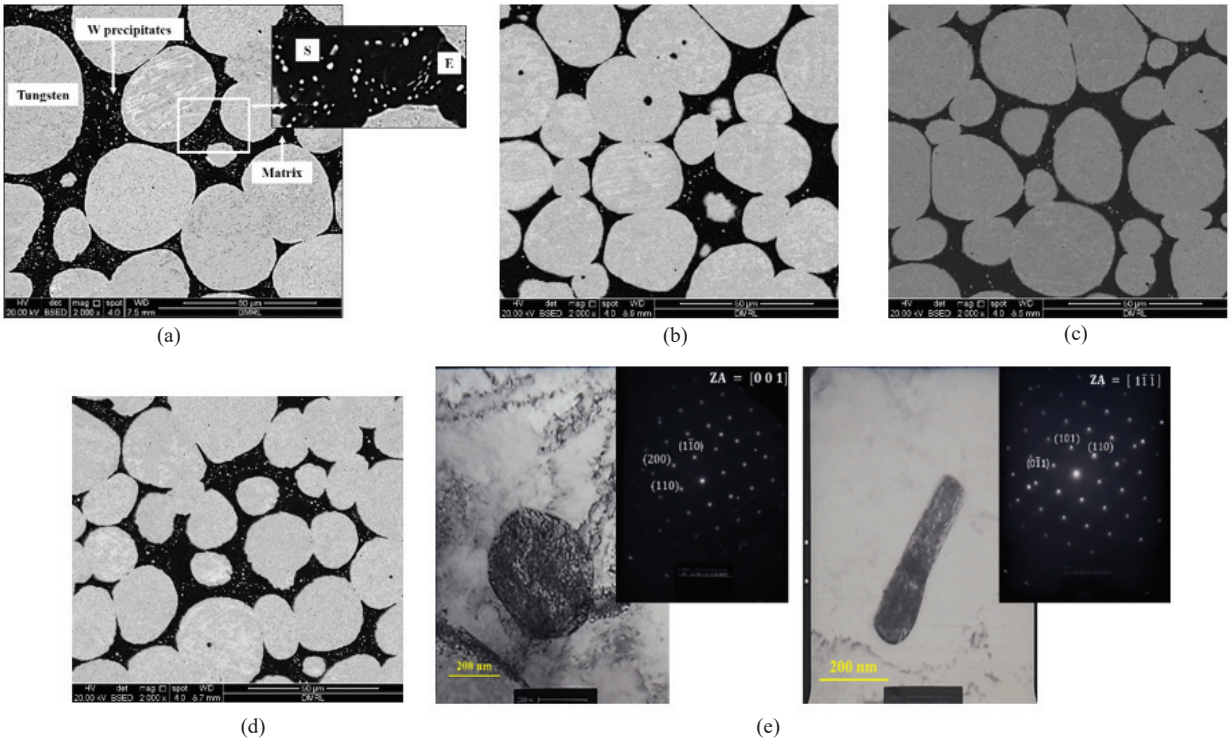

Figure 3. SEM images (taken in BSE mode) of 92W alloy after CHT as in Fig.1a. Second stage temperature in CHT is (a) 1050˚C (Inset: S-nearly-spherical and E-elongated precipitates) (b) 1100˚C (c) 1150˚C and (d) 1150˚C (2 cycles). Fig.3(e) shows bright field TEM images of nearly-spherical and elongated morphologies of the precipitates and corresponding SAD pattern obtained from the precipitates.

Table 4. Microstructural features and mechanical properties in VHT 1 condition. Second stage temperature of CHT carried out prior to VHT 1 is also indicated

Process	Microstructural parameters after VHT 1			Mechanical properties after VHT1		
CHT + VHT 1	Grain size (μm)	Matrix vol. fraction (vol.%)	Vol. fraction of precipitates (%)	Avg. UTS (MPa)	Avg. %El.	Avg. Impact toughness (J/cm^2)
1050˚C/5h	27.8 ± 9.3	23.4 ± 2.1	2.9 ± 0.8	962 ± 5.7	7.5 ± 2.1	97.5 ± 9.2
1100˚C/5h	23.9 ± 9.5	20.2 ± 3.1	1.9 ± 0.8	997 ± 7.1	11 ± 2.1	144 ± 5.7
1150˚C/5h	25.6 ± 11.1	20.2 ± 3.2	1.7 ± 0.4	1010 ± 1.4	15 ± 1.4	142.5 ± 6.4
1150˚C/5h (2 cycles)	25.3 ± 10.4	20.1 ± 2	3.8 ± 0.1	1016 ± 5.7	15.5 ± 1.0	152 ± 2.8

Table 5. Microstructural features and mechanical properties in VHT 2 condition. Second stage temperature of CHT carried out prior to VHT 2 is also indicated

Process	Microstructural parameters			Mechanical properties		
CHT + VHT 2	Grain size (μm)	Matrix vol. fraction (vol.%)	Vol. fraction of precipitates (%)	Avg. UTS (MPa)	Avg. %El.	Avg. Impact toughness (J/cm^2)
1050˚C/5h	26.7 ± 8.3	18.5 ± 3.3	2.3 ± 0.3	1026.5 ± 6.4	18 ± 1.4	107.5 ± 0.7
1100˚C/5h	24.5 ± 10.5	19.6 ± 2.2	1.6 ± 0.3	1023 ± 4.2	17.5 ± 2.1	147.5 ± 4.9
1150˚C/5h	24 ± 10.8	19.1 ± 3.4	1.3 ± 0.1	1024 ± 2.8	16.5 ± 2.1	145 ± 5.7
1150˚C/5h (2 cycles)	24.1 ± 10.7	21.4 ± 2.1	3.5 ± 0.5	1027.5 ± 7.8	15 ± 2.8	178 ± 4.2

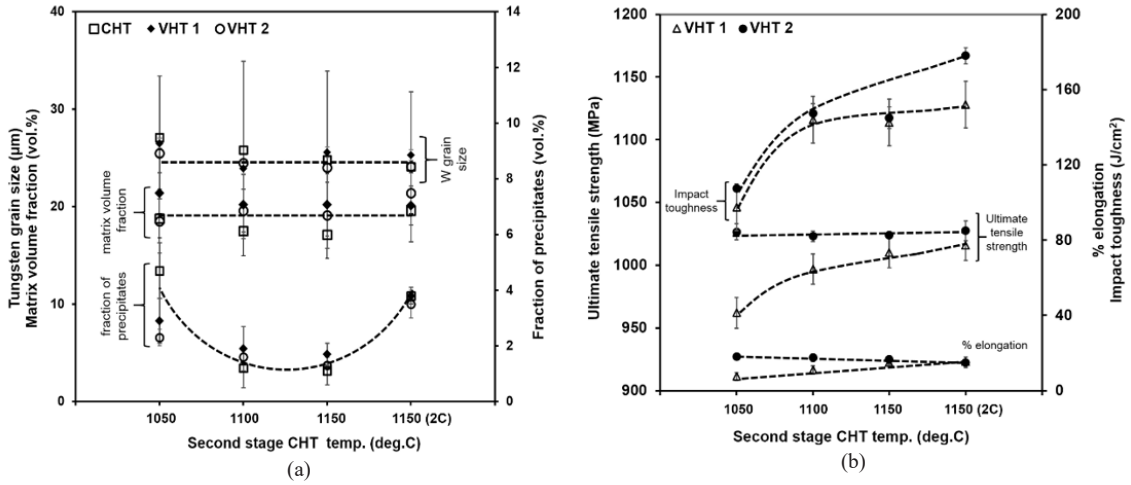

(a) (b)

Figure 4. (a) Microstructural features such as tungsten grain size, matrix volume fraction and volume fraction of precipitates determined after CHT, VHT 1 and 2. Decrease in volume fraction of precipitates following VHT 1 and 2 is shown by arrow and (b) Mechanical properties evaluated after VHT 1 and 2.

1050˚C CHT sample. On the other hand, in other three cases, it is almost similar as compared to CHT (Fig. 4a).

Tensile properties and Charpy unnotched impact toughness evaluated after VHT 1 and 2 are listed in Table 4 and 5. VHT 2 results in superior properties compared to VHT 1 as shown in Fig. 4b. It is also observed that for VHT 1, increasing the second stage temperature leads to improvement in properties whereas no such improvement is observed in VHT 2. VHT 2 gives the best balance of tensile strength, % elongation to failure and impact toughness.

Tensile fractographs of (i) 800˚C-1050˚C-VHT 1 and (ii) 800˚C -1050˚C -VHT 2 are compared in Figs. 5a and 5b. VHT 1 sample shows predominantly intergranular failure (Fig. 5a) whereas both intergranular and transgranular features are seen in VHT 2 sample as in Fig. 5b. This is in agreement with the superior properties of VHT 2 samples as shown in Fig. 4b. Impact fractographs follow a similar trend. Quantitative fractography carried out using tensile and impact fractographs, as shown in Figs. 5c to 5e, indicates that features of intergranular failure are dominant in VHT 1 sample which shows inferior properties compared to VHT 2 sample.

4. DISCUSSION

4.1 Processing

Stuitje[2], *et al.* have reported the temperature range of CHT as 800 to 1050ºC for the first stage and 1100 to 1200ºC for the second stage. In the present study, DSC of as-sintered 92W alloy has been carried out in order to determine the temperature range for CHT and the corresponding phase transitions. Three distinct peaks are observed in the DSC trace as shown in Fig. 2;

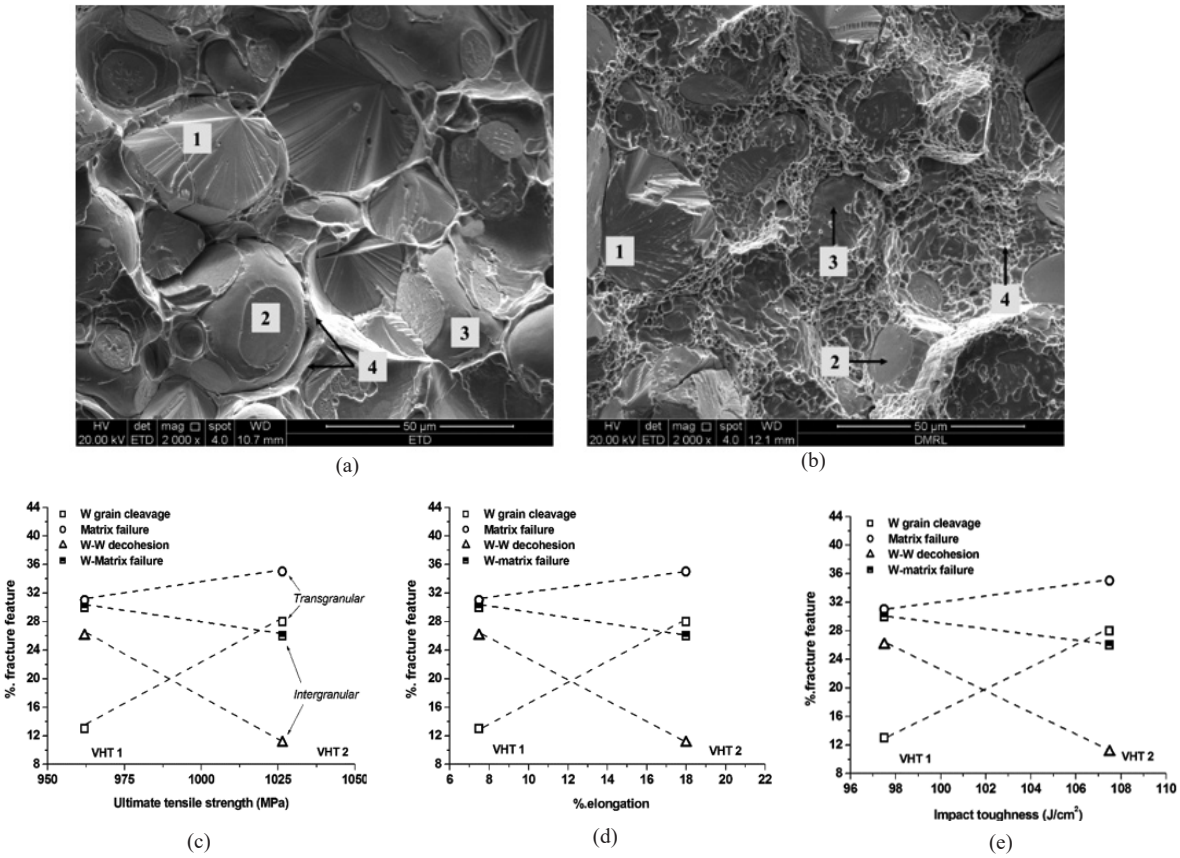

Figure 5. Tensile fractographs of (a) 800˚C-1050˚C-VHT 1 and (b) 800˚C-1050˚C-VHT 2 samples. Features marked are (1) W grain cleavage, (2) W-W decohesion, (3) W-Matrix failure and (4) Matrix failure. VHT 1 sample shows matrix failure by shear lip (4) whereas ductile dimple failure of the matrix (4) is observed in VHT 2 sample. Tensile and impact properties as a function of percentage of intergranular and transgranular failure are shown in (c) to (e).

first peak which is exothermic, ranges from 690 to 870ºC and corresponds to the formation of the intermetallic phase. Formation of intermetallic phase around 800ºC has been reported in our previous investigation[5]. Sarkar[4], *et al.* have reported the intermetallic phase to be Co_2W. Zhang[6], *et al.* have also reported a broad exothermic peak that corresponds to the formation of an intermetallic phase (Fe_6W_6C) in the DSC trace of milled 93W-4.9Ni-2.1Fe alloy. The second peak which is endothermic, ranges from 1014 to 1070ºC and corresponds to the dissolution of the intermetallic phase in the matrix. Thus, the DSC results are consistent with the work of Stuitje[2], *et al.* The third endothermic peak around 1250ºC is possibly due to dissolution of impurity atoms at W-matrix interface. In the present study, first stage of CHT has been fixed at 800ºC/5h based on our previous study and the second stage temperature has been varied as listed in Table 1, in order to understand the changes in microstructural features especially, tungsten precipitates and mechanical properties.

Though Stuitje[2], *et al.* suggest quenching after the second stage of CHT in order to avoid re-formation of the intermetallic phase, furnace cooling has been carried out in the present study. Furnace cooling after second stage of CHT will result in the re-formation of the intermetallic phase and hence a separate vacuum heat treatment has been carried out for a longer duration (4 h) with subsequent oil quenching in order to ensure complete dissolution of the intermetallic phase.

4.2 Microstructural Features

Tungsten grain size determined after CHT, VHT 1 and 2 is between 24 and 28 µm (Table 3 to 5) and is comparable with the grain size reported after liquid phase sintering (23.7 ± 10.5 µm) [5]. This indicates that grain growth has not taken place during CHT irrespective of the second stage temperature or the number of cycles and also during subsequent vacuum heat treatments VHT 1 and 2. This observation is expected, as grain growth by Ostwald ripening mechanism takes place in the presence of liquid matrix during the sintering stage. Since liquid phase does not form in the temperatures used for CHT and VHT 1 and 2, diffusion of tungsten atoms is expected to be slow and hence grain growth is not significant. This is in agreement with the investigation reported by German[7], *et al.* which states that atomic diffusion rate is higher in liquid phase than in solid state.

Volume fraction of precipitates is highest after 1050ºC (Table 3) and includes both nearly-spherical and elongated precipitates within size range of 0.2 - 1.3 µm. Decrease in precipitate fraction after 1100 and 1150ºC is possibly due to the dissolution of very fine precipitates, as the temperature is increased. This is validated by marginal increase in dissolved tungsten which is 42.17 wt% after 1050ºC against 43.35 wt% after 1150ºC. Size of the precipitates after 1100 and 1150ºC does not change significantly and is about 0.5 - 1.3 µm. Volume fraction of precipitates increases again in the case of 1150ºC

(2 cycles) since the instances of intermetallic phase formation and its subsequent dissolution are higher compared to one cycle treatment as in the other three cases. The present study is in agreement with the reported literature which states that increase in number of heat treatment cycles leads to increase in the fraction of precipitates[2].

Volume fraction of precipitates after VHT 1 and 2 is found to decrease only in the case of 1050˚C-VHT (1 and 2) sample as shown in Fig. 4a. As discussed above, dissolution of very fine precipitates at higher temperatures (1100˚C in VHT 1 and 1150 ˚C in VHT 2) due to increased solubility of tungsten in the matrix phase could be the reason behind this trend. Contrarily, fraction of precipitates remains comparable between CHT and VHT (1 and 2) in all the other cases (Fig. 4a). This is because the temperatures of CHT are similar to those of VHT 1 and 2.

4.3 Mechanical Properties

In CHT condition, 92W alloy exhibits ultimate tensile strength of 785 ± 7 MPa, 2 ± 0.5% elongation and impact toughness of 40 ± 8 J/cm^2. In CHT condition, the alloy is brittle, possibly due to re-formation of the intermetallic phase because of slow (furnace) cooling after second stage treatment. Properties improve only after incorporating VHT with oil quenching, as listed in Table 4 and 5. VHT 2 exhibits superior properties compared to VHT 1 as shown in Fig. 4b. A 3-D Plot between tensile strength, elongation and impact toughness (Fig. 6) shows that VHT 2 samples exhibit superior combination of properties compared to VHT 1 and this can be understood from fractographic studies (Figs. 5a to 5e)

From Fig. 5c to 5e it is observed that W grain cleavage and matrix failure (features of transgranular failure) are dominant in VHT 2 sample. More instances of tungsten grain cleavage point towards higher strength and elongation as observed in VHT 2, due to delayed failure of the matrix. In contrast, W-W decohesion and W-matrix failure (features of intergranular failure) are dominant in VHT 1 sample indicating that brittle failure has taken place almost immediately after crack initiation. Hence, VHT 1 sample presents inferior tensile properties. This correlation between mechanical properties and fracture behaviour has been substantiated by several investigations reported on tungsten heavy alloys[8,9]. In the case of impact toughness, ductile-dimple failure of the matrix is expected to result in higher toughness compared to shear lip failure of the matrix. Panchal[9], *et al.* have stated that ductile failure by micro-void coalescence involves higher energy consumption compared to shear lip failure which is expected to be a low energy process. In the present study, VHT 2 sample exhibits ductile dimple failure and hence presents higher impact toughness compared to VHT 1 sample.

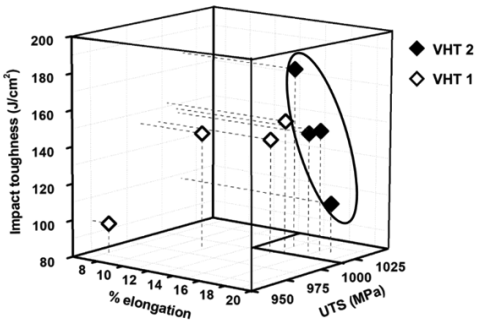

Figure 6. 3-D plot of mechanical properties in VHT 1 and 2 condition.

5. CONCLUSIONS

Effect of cyclic heat treatment and subsequent vacuum heat treatment on the microstructure and mechanical properties of WNiCo alloy has been studied in detail. Major conclusions are as follows;

(i) Volume fraction of tungsten precipitates in the matrix phase during cyclic heat treatment depends on the temperature (for a given soaking time of 5 h) of cyclic heat treatment and the number of cycles.

(ii) Mechanical properties improve only after incorporating vacuum heat treatment with oil quenching.

(iii) Cyclic heat treatment with two continuous cycles followed by vacuum heat treatment at 1150˚C results in the best combination of tensile strength, % elongation to failure and impact toughness. This is attributed to predominant tungsten cleavage and ductile matrix failure.

REFERENCES

1. Prabhu, G., Kumar, Arockia R & Nandy, T.K. Effect of yttrium oxide dispersion on the microstructure and properties of tungsten heavy alloys. *Def. Sci. J.,* 2018, **68**(4), 406-411. doi: 10.14429/dsj.68.12255
2. Stuitje, P.; Harkema, R & Cornelia, T. Heavy metal alloy and method for its production. US Patent No.5462576, 31 October 1995.
3. Skoczylas, P.; Gulbinowicz, Z.; Goroch, O.; Barcz, K & Kaczorowski, M. Research into the production of tungsten heavy alloys with specific mechanical properties. *Probl. Mechatron.; Armnt., Aviat., Saf. eng.,* 2019, **4**(38), 23-36. doi:10.5604/01.3001.0013.6483
4. Sarkar, R.; Singh, V.; Kumar, S.; Rao, Y.V.; Ghosal, P & Nandy, T.K. Structure and orientation of an intermetallic phase in a W-Ni-Co alloy. *Philos. Mag.,* 2019, **99**, 1240-1258. https://doi.org/10.1080/14786435.2019.1579376
5. Prabhu, G., Kumar, Arockia R. & Nandy, T.K. Effect of cyclic heat treatment on the microstructure and mechanical properties of W-Ni-Co alloys. *Int. J. Refract. Met. Hard Mater.,* 2019, **82**, 31-42. doi: 10.1016/j.ijrmhm.2019.03.024
6. Zhang ZW.; Jing-En Z, Xi S, Ran G, Li P. Phase transformation and thermal stability of mechanically alloyed W–Ni–Fe composite materials. *Mater. Sci. Eng. A.,* 2004, **379**(1-2), 148-153. doi: 10.1016/j.msea.2004.02.039
7. German, R.M.; Suri, P. & Park, S.J. Review: liquid phase sintering. *J. Mater. Sci.,* 2009, **44,** 1-39. doi: 10.1007/s10853-008-3008-0
8. Das, J.; Appa, Rao G.; Pabi, S.K.; Sankaranarayana, M. & Nandy, T.K. Thermo-mechanical processing, microstructure and tensile properties of a tungsten heavy alloy. *Mater. Sci. Eng, A.*, 2014, **613**, 48-59. doi: 10.1016/j.msea.2014.06.072

9. Panchal, A. & Nandy, T.K. Effect of composition, heat treatment and deformation on mechanical properties of tungsten heavy alloys. *Mater. Sci. Eng. A.,* 2018, **733**, 374-384.
doi: 10.1016/j.msea.2018.07.070

ACKNOWLEDGEMENTS

The authors would like to thank Defence Research and Development Organisation (DRDO) for sponsoring the activity through a research project. The authors are thankful to the Director, Defence Metallurgical Research Laboratory (DMRL) for his encouragement and guidance. We also thank all the technical staff of DMRL for their valuable contributions.

CONTRIBUTORS

Mr G. Prabhu, Scientist E, obtained his BE (Metallurgical Engineering) from National Institute of Technology, Tiruchirapalli, in 2004 and is currently pursuing PhD from National Institute of Technology, Warangal. He joined DMRL in 2005 and is currently the Group Head of the Powder Metallurgy Group. His research areas include powder metallurgical processing of tungsten, tungsten heavy alloys and microwave sintering.
In the current study, he has contributed in (i) processing of WNiCo alloy by Powder metallurgy route which includes mixing, compaction, sintering and heat treatment, (ii) characterisation which includes sample preparation and microstructure analysis and (iii) evaluation of mechanical properties.

Dr R. Arockia Kumar, obtained his PhD from KAIST, South Korea, in 2010. He had served as a Post-Doctoral Researcher in KAIST, South Korea and in NIMS, Japan. Presently he is working as an Assistant Professor at Department of Metallurgical and Materials Engineering, National Institute of Technology, Warangal. His areas of interest include: Physical metallurgy, phase transformations, shape memory alloys, severe plastic deformation, grain boundary engineering and friction stir processing.
In the current study, he has contributed in detailed characterisation of the alloys including fractography and image analysis.

Dr T.K. Nandy, obtained his PhD in Metallurgical Engineering from IT, BHU, in 1999. Currently, he is serving as the head of Directorate of Powder Metallurgy and Materials Characterisation at Defence Metallurgical Research Laboratory, Hyderabad and his research interest includes tungsten heavy alloys, titanium alloys and intermetallics. He has about 100 papers in refereed journals to his credit and is a life member of IIM. He is the recipient of *DRDO's Agni award of excellence.* In the current study, he has guided in designing experimental work, characterisation and in review of the manuscript.